X-ray Photoelectron Spectroscopic Studies on Organic Photoconductors: Evaluation of Atomic Charges on Chlorodiane Blue and *p*-(Diethylamino)benzaldehyde Diphenylhydrazone

R. J. Waltman* and J. Pacansky

IBM Almaden Research Center, 650 Harry Road, San Jose, California 95120-6099

C. W. Bates, Jr.

Department of Materials Science & Engineering, Stanford University, Stanford, California 94305

Received August 3, 1993®

Atomic charges are evaluated for molecules used in organic photoconductor applications, the carrier-generation molecule chlorodiane blue (CDB) and the hole-transport molecule *p*-(diethylamino)benzaldehyde diphenylhydrazone (DEH). Atomic charges are evaluated from experimental X-ray photoelectron spectroscopic data via a fit to an electrostatic potential model and compared to ab initio population analyses using Mulliken, natural orbital, and CHELPG methods and semiempirical CNDO. The observed chemical shifts in the experimental core level binding energies are correlated to the computed atomic charges.

Introduction

Most printers and photocopiers today utilize an electrophotographic process to produce printed material. For the electrophotographic process to operate efficiently, organic photoconductors in a layered architecture (Figure 1) were invented. A detailed description of organic photoconductors has been given previously.[1] In the layered architecture, an important interface that occurs is that between the charge-generation and charge-transport layers. Here the photogenerated carriers, holes in this case, must be injected with high efficiency to assist meeting the transit time requirements imposed by the printer or copier to ensure rapid output of printed material. Consequently, at the molecular level, the relative orientation of one molecule to another, for example CDB to DEH, may significantly effect the efficiency with which holes are injected from CDB into DEH, as well as the subsequent hopping of the holes (DEH to DEH) in the charge-transport layer.[2] The same CDB/DEH interface is also the origin of an electrical fatigue observed in photoconductors caused by prolonged exposure to long-wavelength light during the electrophotographic cycle.[1,3-5] Apparently, illumination of CDB initiates a solid-state photochemical reaction with DEH resulting in bleaching and depletion of the dye at the interface.[3] Thus, a thorough understanding of the CDB and DEH interface is required, and one method by which insight may be gathered is via molecular modeling. In a forthcoming paper,[6] results of a molecular docking study on CDB and DEH are detailed. Molecular docking studies require reliable atomic charges to effectively model the electrostatic portion of the non-bond-interaction energy and thus provides the motivation for this work. We report herein X-ray photoelectron (XPS) measurements on DEH and CDB. By employing the electrostatic potential model[7] in conjunction with the XPS measurements, atomic charges for DEH and CDB may be obtained. Atomic charges are additionally computed via ab initio quantum chemical methods and compared to the experimentally derived charges. The chemical shifts observed in the core-level binding energies are related to the computed atomic charges.

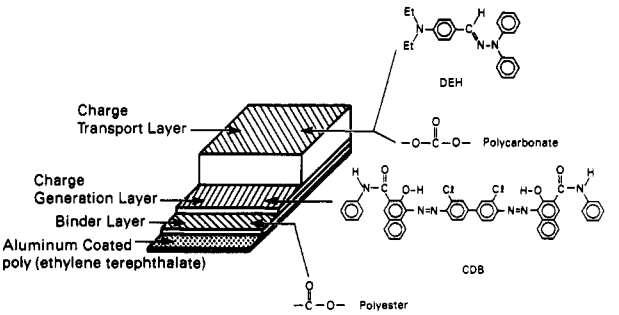

Figure 1. Composition of a layered organic photoconductor.

Experimental Section

XPS measurements on chlorodiane blue were made on a VG Scientific 5000 ESCA spectrometer, and measurements on DEH were made on a Surface Sciences SSX-1150 Model 5. For both, an Al Kα source (E = 1486.7 eV), 20–25 eV pass energy, and 1 × 10^{-9} Torr sample chamber pressure were used. Thin films (1800 Å) of DEH were spin coated from a 3 wt % solution in tetrahydrofuran onto polished and cleaned Si wafers and dried in an oven at 50 °C for 30 min. Samples of chlorodiane blue were

• Abstract published in *Advance ACS Abstracts*, November 1, 1993.

(1) Pacansky, J.; Waltman, R. J.; Grygier, R.; Cox, R. *Chem. Mater.* **1990**, *3*, 454.
(2) Slowik, J. H.; Chen, I. *J. Appl. Phys.* **1983**, *54*, 4467.
(3) Pacansky, J.; Waltman, R. J.; Cox, R. *Chem. Mater.* **1990**, *3*, 903.
(4) Pacansky, J.; Waltman, R. J. *Chem. Mater.* **1990**, *3*, 912.
(5) Pacansky, J.; Waltman, R. J. *Chem. Mater.* **1991**, *3*, 912.
(6) Pacansky, J.; Berry, R. J.; Waltman, R. J., manuscript in preparation.
(7) Siegbahn, K.; Nordling, C.; Johansson, G.; Hedman, J.; Heden, P. F.; Hamrin, K.; Gelius, U.; Bergmark, T.; Werme, L. O.; Manne, r.; Baer, Y. *ESCA Applied to Free Molecules*; North-Holland Publishing Co.: Amsterdam, London, 1969.

0897-4756/93/2805-1799$04.00/0

spin coated (2000 Å) from a 3 wt % solution of CDB in ethylene diamine and dried (in the dark) at 50 °C for 1 week, exposed to tetrahydrofuran to ensure the hydrazone form of the dye,[8] and dried additionally for 1 week. The XPS survey scans revealed no additional elements beyond the expected carbon and nitrogen atoms; for example, no oxygen or silicon substrate signals were observed. As a check for radiation damage during the measurements, the constancy of the ratios of the core level peak intensities and positions were taken as evidence that no significant radiation damage occurred. All binding energies were referenced to the lowest energy C_{1s} line at 284.6 eV.[9] The magnitude of the charge correction was 0.1 eV for chlorodiane blue and 0.2 eV for DEH. XPS elemental compositions are as follows: DEH, 0.886 C, 0.114 N (formula 0.885 C, 0.115 N); CDB, 0.795 C, 0.085 N, 0.061 O, 0.055 Cl (formula 0.793 C, 0.103 N, 0.069 O, 0.034 Cl).

Computational Details

Ab initio calculations on DEH and HCDBH, the hydrazone form of half of a CDB molecule were performed using the IBM/AIX G92RevC version of the Gaussian 92 computer code,[10] using IBM RISC 6000 computers. The geometries were optimized using the 3-21G basis set,[11] with a requested convergence on the SCF density matrices of 10^{-9} and residual forces of $\leq 3 \times 10^{-4}$ hartree/bohr on the Cartesian components. Hessians were computed for DEH (but not for HCDBH) by differentiation of the energy gradient at the optimized geometry; no imaginary frequencies were obtained. The 3-21G optimized geometries and atom numbering schemes are illustrated in Figure 2. HCDBH was used to model CDB (shown in Figure 1) to facilitate the computations. All of the atomic charges reported here were computed at the 3-21G optimized geometries.

Results and Discussion

The solid state XPS core ionization lines for DEH are shown in Figure 3 as an illustrative example. A summary of the experimental and computed (gas phase 3-21G) core-level C_{1s} and N_{1s} binding energies for DEH and HCDBH and additionally O_{1s} and Cl_{2p} binding energies for HCDBH, are summarized in Tables I and II, respectively. In DEH (Figure 3), the C_{1s} envelope contains the CC main line at 284.6 eV and the CN line at 285.8 eV. Additionally, two $\pi \rightarrow \pi^*$ shakeup transitions at 288 and 292 eV were observed as is characteristic of aromatic molecules. The N_{1s} envelope was assigned three binding energies guided by theoretical results, discussed below, and identified via peak fitting at 399.3, 399.9, and 400.3 eV. The core-level binding energies for DEH and HCDBH were also computed via ab initio theory at 3-21G to assist identification of the atoms responsible for ionization. Here the core-level binding energies are the one-electron orbital energies via Koopmans theorem, and the binding energies are assigned to each atom based upon contributions to the molecular orbital of the 1s (C, N, O) and 2p (Cl) wave functions from the Mulliken 3-21G population analyses.

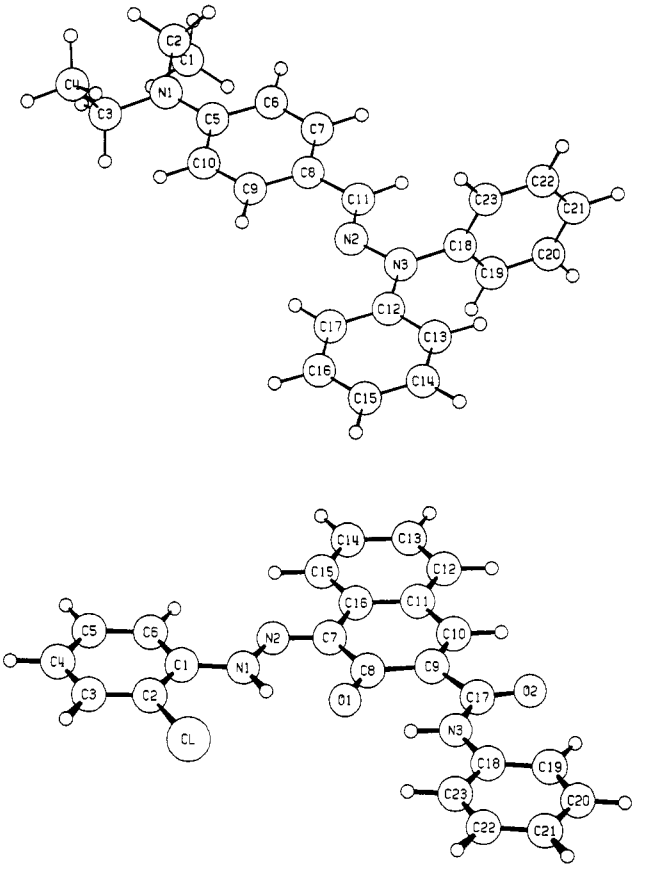

Figure 2. SCF 3-21G optimized geometries for DEH (top) and HCDBH (bottom). Total energies are −1 042.989 448 and −1 644.004 699 hartrees for DEH and HCDBH, respectively.

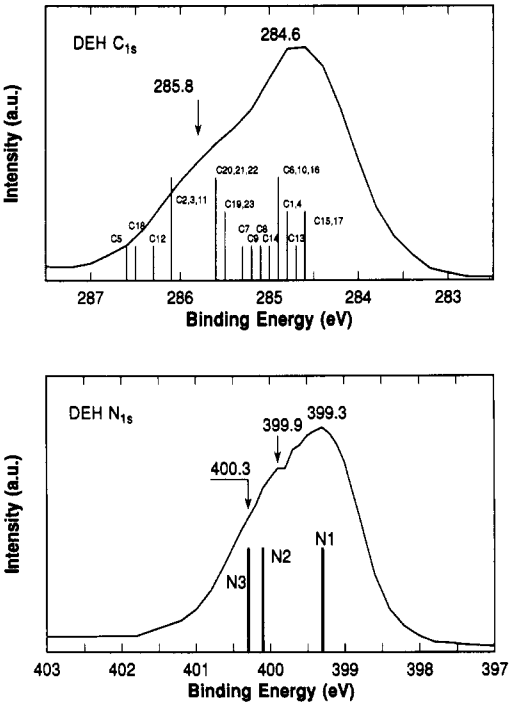

Figure 3. XPS core ionization spectra for DEH. The lines under the experimental envelopes are the binding energies computed by SCF 3-21G.

All of the computed binding energies are assigned to atom type and summarized in Tables I and II, and are plotted underneath the experimental envelopes (Figures 3 and 5). The computed binding energies were scaled uniformly to match the experimental binding energies by taking the

(8) Pacansky, J.; Waltman, R. J. *J. Am. Chem. Soc.* **1992**, *114*, 5813.
(9) Barth, G.; Linder, R.; Bryson, C. *Surf. Interface Anal.* **1988**, *11*, 307.
(10) Gaussian 92, Revision C; Frisch, M. J.; Trucks, G. W.; Head-Gordon, M.; Gill, P. M. W.; Wong, M. W.; Foresman, J. B.; Johnson, B. G.; Schlegel, H. B.; Robb, M. A.; Replogle, E. S.; Gomperts, R.; Andres, J. L.; Raghavachari, K.; Binkley, J. S.; Gonzalez, C.; Martin, R. L.; Fox, D. J.; Defrees, D. J.; Baker, J.; Stewart, J. J. P.; Pople, J. A. Gaussian, Inc.: Pittsburgh, PA, 1992.
(11) (a) Binkley, J. S.; Pople, J. A.; Hehre, W. J. *J. Am. Chem. Soc.* **1980**, *102*, 939. (b) Gordon, M. S.; Binkley, J. S.; Pople, J. A.; Pietro, W. J.; Hehre, W. J. *J. Am. Chem. Soc.* **1982**, *104*, 2797.

Table I. Atomic Charges and Core-Level N_{1s} and C_{1s} Binding Energies for DEH (The Atom Numbering Scheme Refers to Figure 2)

	q, atomic charges						E_b (eV), binding energies		
atom	Mulliken STO-3G	Mulliken 3-21G	nat Orb 3-21G	CHELPG 3-21G	CNDO	XPS	XPS	3-21G	$\Sigma(q_j/r_{ij})$ (eV)
N1	−0.293	−0.941	−0.561	−0.622	−0.268	−0.075	399.3	399.3	0.98
N2	−0.148	−0.360	−0.269	−0.286	−0.118	+0.087	400.2	400.1	−1.11
N3	−0.217	−0.876	−0.375	−0.263	−0.211	−0.024	399.9	400.3	+0.65
C1	−0.184	−0.594	−0.680	−0.232	−0.119	+0.027	284.6	284.8	−0.80
C2	+0.002	−0.168	−0.212	+0.241	+0.088	+0.208	285.8	286.1	−3.70
C3	+0.002	−0.168	−0.212	+0.262	+0.088	+0.208	285.8	286.1	−3.70
C4	−0.184	−0.594	−0.680	−0.213	−0.119	+0.027	284.6	284.8	−0.80
C5	+0.129	+0.466	+0.269	+0.545	+0.175	+0.254	285.8	286.6	−4.73
C6	−0.102	−0.281	−0.331	−0.411	−0.075	+0.023	284.6	284.9	−0.72
C7	−0.053	−0.199	−0.167	−0.084	+0.001	+0.066	284.6	285.3	−1.70
C8	−0.022	−0.191	−0.181	−0.084	−0.002	+0.052	284.6	285.1	−1.38
C9	−0.048	−0.180	−0.150	−0.036	+0.002	+0.074	284.6	285.2	−1.89
C10	−0.101	−0.281	−0.325	−0.401	−0.075	+0.023	284.6	284.9	−0.72
C11	+0.024	+0.199	+0.072	+0.266	+0.095	+0.177	285.8	286.1	−3.01
C12	+0.130	+0.438	+0.234	+0.266	+0.164	+0.235	285.8	286.3	−4.30
C13	−0.095	−0.284	−0.309	−0.268	−0.074	+0.013	284.6	284.7	−0.49
C14	−0.056	−0.219	−0.208	−0.034	+0.006	+0.069	284.6	285.0	−1.77
C15	−0.084	−0.268	−0.290	−0.257	−0.046	+0.035	284.6	284.6	−1.00
C16	−0.057	−0.220	−0.209	−0.061	+0.005	+0.072	284.6	284.9	−1.84
C17	−0.085	−0.266	−0.290	−0.222	−0.068	+0.038	284.6	284.6	−1.07
C18	+0.099	+0.267	+0.127	+0.612	+0.147	+0.206	285.8	286.5	−3.65
C19	−0.062	−0.213	−0.220	−0.282	−0.051	+0.019	284.6	285.5	−0.64
C20	−0.064	−0.242	−0.244	−0.110	−0.006	+0.053	284.6	285.6	−1.40
C21	−0.059	−0.234	−0.229	−0.171	−0.027	+0.053	284.6	285.6	−1.40
C22	−0.064	−0.242	−0.244	−0.100	−0.007	+0.047	284.6	285.6	−1.27
C23	−0.062	−0.213	−0.220	−0.295	−0.051	+0.020	284.6	285.5	−0.65

Table II. Atomic Charges and Core-Level N_{1s}, C_{1s}, O_{1s}, and Cl_{2p} Binding Energies for CDB (The Atom Numbering Scheme Refers to Figure 2)

	q, atomic charges						E_b (eV), binding energies		
atom	Mulliken STO-3G	Mulliken 3-21G	nat Orb 3-21G	CHELPG 3-21G	CNDO	XPS	XPS	3-21G	$\Sigma(q_j/r_{ij})$ (eV)
N1	−0.263	−0.775	−0.466	−0.200	−0.242	−0.128	400.1	402.0	+2.77
N2	−0.100	−0.368	−0.122	−0.136	−0.052	+0.071	400.1	402.6	−0.92
N3	−0.383	−1.128	−0.734	−0.924	−0.383	−0.241	400.1	400.1	+4.86
O1	−0.275	−0.696	−0.649	−0.590	−0.377	−0.173	533.4	532.9	+3.59
O2	−0.295	−0.670	−0.686	−0.670	−0.395	−0.286	531.4	531.4	+3.11
Cl	−0.173	+0.112	−0.045	−0.169	−0.177		200.7	200.7	
							202.3	200.8	
C1	+0.135	+0.473	+0.191	+0.266	+0.172	+0.197	286.2	287.5	−3.06
C2	+0.036	−0.349	−0.077	−0.046	+0.034	+0.037	284.6	287.6	−1.04
C3	−0.050	−0.178	−0.216	−0.039	+0.006	+0.032	284.6	286.2	−0.91
C4	−0.067	−0.246	−0.258	−0.224	−0.036	+0.010	284.6	285.7	−0.44
C5	−0.050	−0.225	−0.208	−0.060	+0.008	+0.039	284.6	285.9	−1.09
C6	−0.070	−0.237	−0.264	−0.258	−0.058	+0.002	284.6	285.8	−0.24
C7	+0.043	+0.320	+0.048	−0.044	+0.037	+0.091	286.2	287.1	−0.66
C8	+0.183	+0.591	+0.577	+0.762	+0.290	+0.343	287.7	288.8	−4.85
C9	−0.063	−0.320	−0.311	−0.566	−0.114	−0.089	284.6	286.0	+1.81
C10	−0.021	−0.064	−0.009	−0.011	+0.025	+0.047	284.6	286.7	−1.25
C11	−0.015	−0.136	−0.134	+0.072	+0.000	+0.017	284.6	286.2	−0.59
C12	−0.052	−0.182	−0.172	−0.201	−0.011	+0.029	284.6	286.0	−0.85
C13	−0.067	−0.244	−0.253	−0.124	−0.026	+0.023	284.6	285.7	−0.72
C14	−0.054	−0.213	−0.199	−0.082	−0.006	+0.038	284.6	285.9	−1.06
C15	−0.064	−0.199	−0.221	−0.156	−0.033	+0.013	284.6	285.7	−0.49
C16	+0.017	−0.049	−0.014	+0.028	+0.036	+0.032	284.6	286.5	−0.93
C17	+0.306	+1.046	+0.807	+1.044	+0.455	+0.493	287.7	288.6	−8.24
C18	+0.124	+0.383	+0.204	+0.561	+0.172	+0.253	286.2	286.3	−4.32
C19	−0.093	−0.265	−0.279	−0.340	−0.070	−0.011	284.6	284.6	+0.05
C20	−0.056	−0.228	−0.217	−0.050	+0.002	+0.042	284.6	284.9	−1.16
C21	−0.079	−0.256	−0.270	−0.231	−0.041	+0.012	284.6	285.0	−0.46
C22	−0.058	−0.225	−0.219	−0.031	+0.002	+0.039	284.6	284.9	−1.07
C23	−0.086	−0.270	−0.281	−0.413	−0.070	+0.009	284.6	284.9	−0.40

smallest orbital energy for each element and scaling it to the smallest experimentally observed core binding energy. The scaling factors for both DEH and HCDBH were 0.94 and 0.95 for the C_{1s} and N_{1s} orbital energies, respectively, and additionally for HCDBH, 0.96 and 0.93 for the O_{1s} and Cl_{2p} orbital energies, respectively. As an illustrative example, the computed 3-21G orbital plots of the N_{1s} wave functions and their corresponding binding energies are displayed in Figure 4 for DEH. The orbital plots facilitate the assignment of the binding energies to the specific atoms ionized. On the basis of the molecular orbital plots, the aniline amine nitrogen atom N1 has the smallest N_{1s} binding energy, 399.3 eV, while the imine N2 and hydrazone amine N3 have similar binding energies, 400.1 and 400.3 eV, respectively (Figure 4). For DEH C_{1s}, the computed 3-21G binding energies cluster into two groups near 285 and 286 eV (Figure 3 and Table I). Those near the 285-eV region are identified with CC bonding while those in the 286-eV region are attributed to CN bonding. Similar results are obtained for HCDBH (Table II, Figure

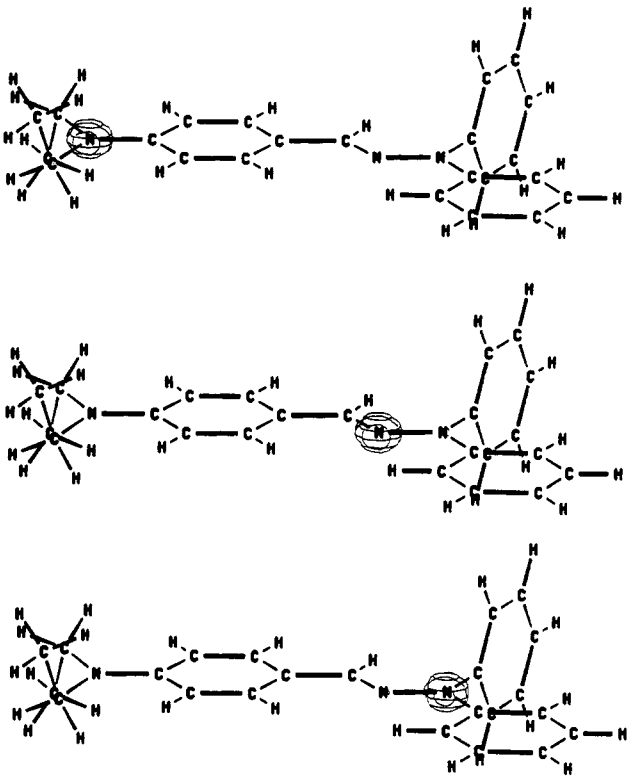

Figure 4. Molecular orbital plots of the N_{1s} wave functions in DEH: (top) N1, E_b = 399.3 eV; (middle) N2, E_b = 400.1 eV; (bottom) N3, E_b = 400.3 eV.

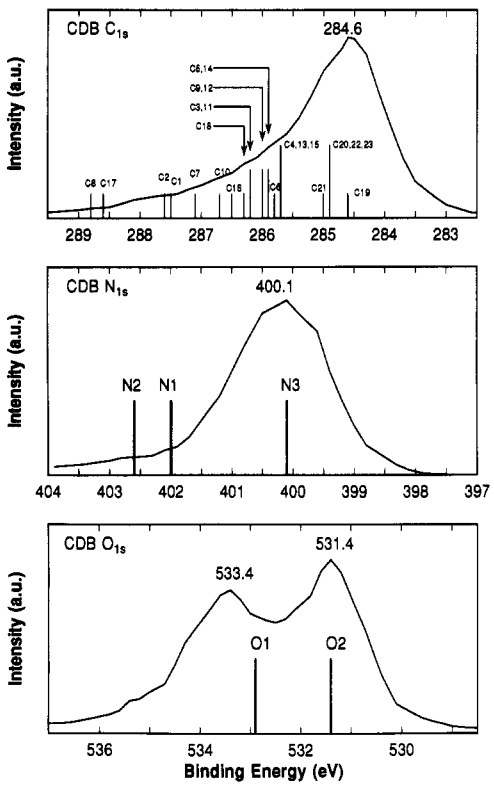

Figure 5. XPS core ionization spectra for CDB. The lines under the experimental envelopes are the binding energies computed by SCF 3-21G.

5). For HCDBH N_{1s} computed at 3-21G, the amido nitrogen atom N3 has the smallest binding energy, 400.1 eV, while the hydrazone quinone nitrogen atoms N1 and N2 have somewhat higher binding energies of 402.0 and 402.6 eV. For HCDBH O_{1s}, the amido oxygen O2 and the naphthyl oxygen O1 have experimental binding energies separated by 2 eV with O1 having the lower binding energy. For HCDBH C_{1s}, the computed 3-21G binding energies cluster into three groups near 285, 287, and 289 eV. Those near the 285-eV region are identified with CC bonding, those in the 286–287-eV region are attributed to CN bonding, and those near 289 eV are due to the very polar CO bonding.

Table III. Atomic Charges for the Hydrogen Atoms on DEH (The Atom Numbering Scheme Refers to Figure 2)

	q, atomic charges				
atom	Mulliken STO-3G	Mulliken 3-21G	nat orb 3-21G	CHELPG 3-21G	CNDO
H (C1)	0.061	0.206	0.226	0.069	0.039
H (C1)	0.061	0.193	0.222	0.054	0.037
H (C1)	0.066	0.219	0.232	0.053	0.041
H (C2)	0.065	0.220	0.226	0.037	0.007
H (C2)	0.070	0.221	0.228	0.002	0.013
H (C3)	0.065	0.220	0.226	0.029	0.007
H (C3)	0.070	0.223	0.229	−0.007	0.013
H (C4)	0.061	0.206	0.225	0.061	0.039
H (C4)	0.061	0.194	0.223	0.047	0.037
H (C4)	0.066	0.220	0.232	0.047	0.041
H (C6)	0.057	0.238	0.236	0.203	0.021
H (C7)	0.059	0.237	0.235	0.135	0.010
H (C9)	0.077	0.268	0.252	0.118	0.017
H (C10)	0.058	0.240	0.237	0.204	0.021
H (C11)	0.059	0.250	0.208	0.018	−0.004
H (C13)	0.062	0.256	0.248	0.064	0.021
H (C14)	0.062	0.234	0.237	0.127	0.010
H (C15)	0.059	0.229	0.236	0.135	0.016
H (C16)	0.063	0.234	0.237	0.123	0.010
H (C17)	0.084	0.273	0.262	0.122	0.032
H (C19)	0.078	0.268	0.257	0.141	0.030
H (C20)	0.070	0.249	0.245	0.141	0.019
H (C21)	0.070	0.247	0.243	0.138	0.019
H (C22)	0.070	0.249	0.245	0.138	0.019
H (C23)	0.078	0.268	0.257	0.146	0.030

Table IV. Atomic Charges for the Hydrogen Atoms on CDB (The Atom Numbering Scheme Refers to Figure 2)

	q, atomic charges				
atom	Mulliken STO-3G	Mulliken 3-21G	nat orb 3-21G	CHELPG 3-21G	CNDO
H (N1)	0.277	0.465	0.477	0.308	0.239
H (N3)	0.242	0.425	0.458	0.422	0.207
H (C3)	0.036	0.282	0.266	0.148	0.046
H (C4)	0.076	0.257	0.251	0.153	0.032
H (C5)	0.077	0.257	0.249	0.137	0.027
H (C6)	0.092	0.285	0.265	0.164	0.041
H (C10)	0.101	0.323	0.279	0.175	0.046
H (C12)	0.072	0.261	0.248	0.165	0.024
H (C13)	0.070	0.254	0.249	0.130	0.024
H (C14)	0.070	0.255	0.247	0.132	0.020
H (C15)	0.080	0.274	0.256	0.115	0.021
H (C19)	0.094	0.307	0.280	0.198	0.060
H (C20)	0.064	0.240	0.240	0.120	0.013
H (C21)	0.061	0.234	0.238	0.137	0.017
H (C22)	0.060	0.239	0.240	0.119	0.013
H (C23)	0.060	0.241	0.239	0.206	0.024

Atomic charges are presented in Tables I–IV. At the ab initio level of theory, we report Mulliken charges using STO-3G[12] and 3-21G bases, and natural orbital and CHELPG (charges from electrostatic potential, grid oriented)[13] charges using 3-21G basis. Mulliken charges employ the simplest partioning scheme whereby electrons are equally shared between pairs of functions which

(12) (a) Hehre, W. J.; Stewart, R. F.; Pople, J. A. *J. Chem. Phys.* **1969**, *51*, 2657. (b) Hehre, W. J.; Ditchfield, R.; Stewart, R. F.; Pople, J. A. *J. Chem. Phys.* **1970**, *52*, 2769.

(13) (a) Breneman, C. M.; Wiberg, K. B. *J. Comput. Chem.* **1990**, *11*, 361. (b) Chirlian, L. E.; Francl, M. M. *J. Comput. Chem.* **1987**, *8*, 894.

overlap.[14] Because nonorthogonal orbitals are employed, Mulliken analyses, particularly with increasing basis set size, often lead to nonphysical electron distributions. These complications are avoided using orthogonal natural atomic orbitals which show convergence with increasing basis set size.[15,16] It should be noted, however, that Mulliken and natural orbital charges at STO-3G often yield similar results. CHELPG charges, also reported here, are computed based upon a fit to the electrostatic potential field surrounding the molecule.[13] The CHELPG charges computed here were constrained to reproduce the dipole moment of each molecule. Finally, atomic charges using the semiempirical CNDO method[17] are tabulated to provide a more comprehensive analysis of the experimental XPS data. Using an electrostatic potential model,[7] the core binding energies may be related to charge distribution by eq 1, where E_i^{ref} is a reference energy, kq_i represents

$$E_i = E_i^{ref} + kq_i + \sum_{j \neq i} q_j/r_{ij} \quad (1)$$

the potential from the charge on the atom i, and $\sum q_j/r_{ij}$ is an intramolecular Madelung-type potential and represents the potential arising from charges on the other atoms in the molecule. The determination of molecular charge distributions from experimental binding energies using eq 1 requires knowledge of the parameters k and E_i^{ref} for each core level. These parameters have been fit empirically relating CNDO charges to experimental binding energies;[7] thus the charges determined from XPS data are expected to correlate with CNDO charges. We have used the compilations provided by Peeling.[18,19] For C_{1s}, E_i^{ref} = 284.8 eV and k_C = 22.6 eV/unit charge. For N_{1s}, E_i^{ref} = 399.7 eV and k_N = 18.5 eV/unit charge. For O_{1s}, E_i^{ref} = 532.6 eV and k_N = 16.1 eV/unit charge. Other similar values for these parameters have also been reported.[20]

The atomic charges for the heavy atoms are presented in Tables I and II and for hydrogen atoms in Tables III and IV for DEH and HCDBH, respectively. In general, the Mulliken STO-3G, CNDO and XPS charges are considerably smaller in magnitude than the corresponding Mulliken, natural orbital, and CHELPG atomic charges at 3-21G, especially for the polar bonds, e.g., C–O and C–N. Among STO-3G, CNDO, and XPS charges, there is good agreement between STO-3G and CNDO, while the XPS charges are comparatively uniformly more positive, the latter attributed to the approximate nature of eq 1 and the limited reliability of the empirical values of E_i^{ref} and k. More importantly, the relative magnitudes of the atomic charges from XPS, STO-3G, and CNDO correctly account for the experimental chemical shifts observed in the core-level binding energies in DEH and CDB. For example, the amine nitrogen atom N1 in DEH is considerably electron-rich compared to N2 and N3 and on this basis, would be expected to have a relatively lower binding energy. In the C_{1s} spectrum of DEH, the carbon atoms bonded to nitrogen are comparatively electron deficient to C–C carbon atoms; consequently, their core ionization lines are shifted to higher binding energies (Figure 3). The Mulliken and natural orbital atomic charges computed at 3-21G also provide similar relative data; however, slightly different results were obtained from the CHELPG method. While a large negative charge is computed on the aniline amine nitrogen atom N1, the CHELPG model places comparatively smaller charges on N2 and N3 and, moreover, predicts the imine N2 to be very slightly more electron rich than the hydrazone amine N3. In this case the imine N2 would be expected to have a slightly lower N_{1s} binding energy compared to the amine N3, in contrast to the results obtained from all of the other charge determination methods. The CHELPG charges for the carbon atoms C2 and C3 also differ from Mulliken and natural orbital 3-21G charges. These are the diethyl carbon atoms C2 and C3 bonded to the aniline amine N1, which have positive charges from CHELPG but negative charges from Mulliken and natural orbital 3-21G methods. The binding energies computed at 3-21G place the C_{1s} core ionization lines for C2 and C3 at 286.1 eV, considerably higher in energy and consistent with electron-deficient carbon atoms in DEH (Table I, Figure 3). Since the negative end of the C–N dipole is expected to be nitrogen which is more electronegative than carbon, the CHELPG charges here are consistent with CNDO and XPS charges.

Similar results are obtained for HCDBH. Mulliken STO-3G, CNDO, and XPS charges are smaller in magnitude than the corresponding Mulliken, natural orbital, and CHELPG charges at 3-21G. In all cases, the amido nitrogen N3 is more negative than the hydrazone amine N1 and N2 and thus would be expected to have the smallest binding energy; we were not able to achieve a high enough resolution in our XPS spectrum to distinguish the N_{1s} envelope (Figure 5). The oxygen atom O1 is more electron deficient than O2 for all reported charges (except Mulliken 3-21G) and thus has the higher binding energy. Amido oxygens such as O2 have been observed to have lower binding energies than most carbonyl oxygen atoms.[21,22] The carbon atoms bonded to oxygen, C17, and C8, have the highest electron deficiencies and consequently the highest binding energies (C_{1s}, 287.7 eV). The carbon atoms bonded to nitrogen, C1, C7, and C18, are less electron deficient than C–O and are assigned the 286.2-eV experimental binding energy.

Concluding Remarks

For the photoconductor industry to produce more robust organic photoconductors with greater longevity, charge injection efficiencies and hopping conductivity must be maximized, and the photochemically induced damage incurred during the electrophotographic cycle minimized. All of these properties are greatly dependent upon intermolecular orientation between organic molecules, CDB and DEH and/or DEH and DEH contact pairs. Molecular modeling, in particular molecular docking studies, is expected to provide significant insight provided that the parameters used in the modeling are reliable.

(14) Mulliken, R. S. *J. Chem. Phys.* **1955**, *23*, 1833.
(15) Lowdin, P. O. *Phys. Rev.* **1955**, *97*, 1474.
(16) Reed, A. E.; Weinstock, R. B.; Weinhold, F. *J. Chem. Phys.* **1985**, *83*, 735.
(17) Pople, J. A.; Beveridge, D. L. *Approximate Molecular Orbital Theory*; McGraw-Hill: New York, 1970.
(18) Peeling, J.; Hruska, F. E.; McIntyre, N. S. *Can. J. Chem.* **1978**, *56*, 1555.
(19) Peeling, J.; Hruska, F. E.; McKinnon, D. M.; Chauhan, M. S.; McIntyre, N. S. *Can. J. Chem.* **1978**, *56*, 2405.
(20) Clark, D. T., Thomas, H. R. *J. Polym. Sci., Polym. Chem. Ed.* **1978**, *16*, 791.
(21) Clark, D. T.; Thomas, H. R. *J. Polym. Sci., Polym. Chem. Ed.* **1976**, *14*, 1671.
(22) Clark, D. T.; Harrison, A. *J. Polym. Sci., Polym. Chem. Ed.* **1981**, *19*, 1945.

With this goal in mind, we have attempted to evaluate the partial atomic charges on CDB and DEH and correlate the chemical shifts in the XPS binding energies to ascertain some indication of their accuracy. Thus, atomic charges for DEH and HCDBH were determined via XPS measurements in conjunction with the electrostatic potential model and compared to semiempirical CNDO and ab initio Mulliken, natural orbital, and CHELPG methods. The atomic charges determined from the XPS data and the computed Mulliken STO-3G and CNDO provided an accurate description of the observed chemical shifts in the experimental core level binding energies. With increasing size of the basis set to 3-21G, the magnitude of the atomic charges increased, particularly for the polar C–N and C–O bonds; however, the relative charges for the most part correlated with the observed chemical shifts in the experimental core level binding energies. The CHELPG charges provided the best overall agreement to the experimentally observed chemical shifts in the core level binding energies.